Microscopic "Slide-Snap" Receding Contact Line Dynamics on Superhydrophobic Surfaces

Y.H. Yeong[*], A. Milionis[*], I. Bayer[**] and E. Loth[*]

[*]Department of Mechanical & Aerospace Engienering, University of Virginia, VA, USA.
[**]Smart Materials, Central Laboratories, Istituto Italiano di Tecnologia, Genoa, Italy.

ABSTRACT

Receding angles have been shown to have great significance when designing a superhydrophobic surface for applications involving self-cleaning. Although apparent receding angles under dynamic conditions have been well studied, the microscopic receding contact line dynamics are not well understood. Therefore, experiments were performed to measure these dynamics on textured square pillar superhydrophobic surfaces (pillar spacing of 63 μm and 120 μm) at micron length scales and at micro-second temporal scales. Results revealed a consistent "slide-snap" motion of the microscopic receding line as compared to the "stick-slip" dynamics reported in previous studies. Interface angles between 40-60° were measured for the pre-snap receding lines on all pillar surfaces. This is in contrast to the apparent pre-snap receding lines which were observed to range between 120° and 140°.

Keywords: superhydrophobic, receding contact angle, microscopic, contact line dynamics

1 INTRODUCTION

Under the Cassier-Baxter[1] and Wenzel[2] wetting models, the affinity of water to a superhydrophobic surface can be quantified by the water contact angle (CA), an equilibrium angle characterizing the three phase contact line of water, surface and air. However, it has been comprehensively agreed by researchers that the sole use of CA is insufficient to describe the wettability of the surface[3-4], especially within the context of practical applications of superhydrophobic surfaces such as self-cleaning. This was confirmed by Wang *et al.*[5] who reported the possibility of various non-wetting states where the CA's of the surface are high but limited in droplet mobility. It is therefore clear that additional parameters would be required to quantify the state of superhydrophobicity of a surface.

To accomplish this, dynamic angles such as the advancing and receding angles were prescribed.[6-7] Consider the case where a drop rolls on a tilted superhydrophobic surface. For the drop to move forward, the leading edge of the droplet has to advance, creating an angle on the three-phase contact line called the advancing angle. On the other hand, the trailing edge of the drop retreats from the surface to form the receding angle. Both the advancing and receding contact line motions are highly dynamic, transitioning from one metastable state to another and have been extensively studied using theoretical[7-8], experimental[4, 9] and computational methods[10-11]. Researchers have observed that the advancing three-phase contact line on superhydrophobic surfaces consisting of pillar geometries does not move, but rather descends upon its adjacent pillar to wet the top of the pillar surface.[8-10, 12-14] The receding contact line on the other hand is forced to detach from one pillar to another in a discrete fashion, creating a pinning-depinning motion. Although the occurrence of this receding contact line detachment has been well documented,[8-9,13-16] questions still remain on the precise dynamics and degree in which the receding line disjoins from one pillar to another. In fact, researchers have hypothesized conflicting scenarios for the receding mechanism.[7,9,14] Understanding the depinning mechanisms would not only improve our fundamental comprehension of adhesion and wettability of superhydrophobic surfaces at the microscopic level but would also have profound implications on practical applications.

In this study, we present to the best of our knowledge, a first experimental investigation to measure the microscopic receding contact line dynamics of superhydrophobic surfaces with textured pillar surface features at micron length scales and at microsecond temporal resolution. The pillar superhydrophobic surfaces consisted of square micron-sized pillars spaced apart at 63 μm and 120 μm and spray coated with sub-micron PTFE particles. A drop was set in motion on these surfaces so that its three-phase receding contact line dynamics could be recorded using a high speed camera for qualitative and quantitative analysis.

2 EXPERIMENTAL METHODS

2.1 Superhydrophobic Surface Fabrication

The fabrication of the textured pillar surface pillars involved various steps: spin-coating of photoresist SU-8 3050 (Microchem. USA) on a silicon wafer, soft-baking of the material followed by UV exposure with mask aligner, post-exposure baking and finally washed for development. Secondary roughness was then created by spray coating poly(tetrafluoroethylene) (PTFE) sub-micrometer particles, on the pillar tops. The concept of creating secondary roughness on top of a pillar surface for the creation of anti-wetting materials was also used by Steele *et al*.[17] and Cao *et*

al.[18] The existence of these two length scales on the pillar surfaces have been shown to relieve receding contact line pinning[23] and was hence utilized for this experiment. Two superhydrophobic pillar surfaces were fabricated using this method, a surface with inter-pillar distance (L) of 63 µm and one at 120 µm. Contact angles and roll-off angles for both surfaces were above 150° and less than 20°, respectively. Scanning electron microscope (SEM) pictures of a pillar surface at L = 63 µm is shown in Figure 1. Further details about the microfabrication of these superhydrophobic surfaces can be found in Yeong et al.[19]

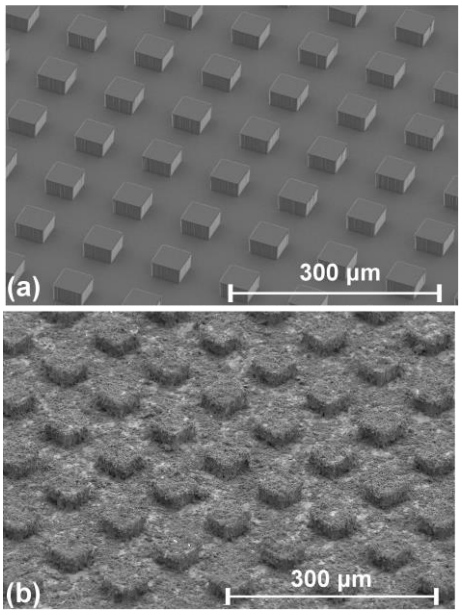

Figure 1: (a) SEM images of a pristine pillar surface at L= 63 µm prior to deposition of PTFE particles (b) superhydrophobic pillar surface after deposition of PTFE particles. (Image acquired from Yeong *et al.*[19])

2.2 Experimental Set-Up

The schematic of the experimental set-up is shown in Figure 2. The experiment method involved placing the textured pillar surface on a high precision rotation stage (PRM-1, Thorlabs, USA) and manually tilting it at an approximate rate of 3.5 degrees/s to allow a water drop (10 µL) to roll from the surface. High magnification optics coupled with high-speed imagery was utilized to record the dynamics of the microscopic receding angle while the droplet was traveling down the inclination. This was accomplished by attaching a microscope lens (6.5X UltraZoom fine focus with 2X F-mount adapter and 2X Lens attachment, Navitar, USA) to a high-speed camera (Fastcam SA-4, Photron, Japan). Under the back-lighting of a high intensity fiber optic illuminator (MI-150, Dolan-Jenner, USA) and through the aperture of the rotating stage, high contrast images of the microscopic receding contact line motions on each pillar were acquired at 15,000 frames/s (66 µs between each frame), with a resolution of 193 × 181 pixels for each frame. The entire set-up was constructed on top of an optical table to reduce external vibrations that could potentially introduce noise to the measurements. The contact line motions were recorded over 4 pillars for each of the four textured pillar surfaces of different inter-pillar distances. The recordings were then repeated at a different locations on the substrate.

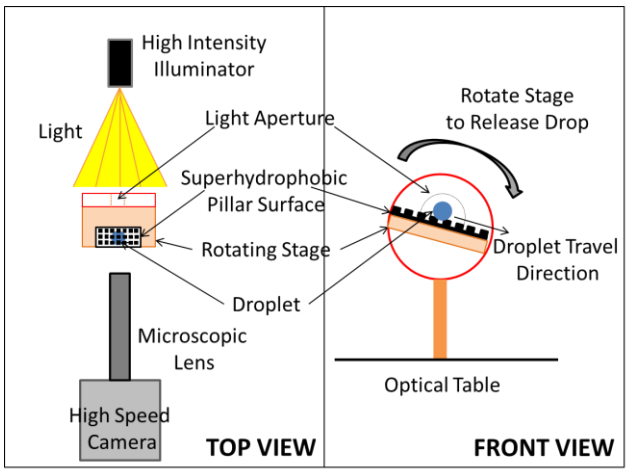

Figure 2: Schematic of the experimental setup (Image acquired from Yeong *et al.*[19])

3 RESULTS & DISCUSSION

Figure 3 shows the images depicting the initial (0 to 0.2 ms shown in left column of Figure 3) and final events (1.06 to 1.26 ms shown in right column of Figure 3) of the receding line motion on a single pillar for a surface with a L value of 63 µm. The total duration of the receding line motion on the pillar is 1.26 ms. These images represent the key events during a single cycle of dynamic interaction between the receding line and the pillar. It can be observed that the receding line was initially (at t=0 s) relaxed and had a high contact angle. However, it rapidly (within 0.13 ms) transitioned into a stage where the contact line was stretched and pulled inwards to form a concave shape as it traversed across the top of the pillar surface. The travel of the receding line between the duration of 0.26 ms and 1 ms was however limited, and only occurred over a small interface distance. Necking of the receding contact line would eventually start to occur after t=1 ms with the formation of instabilities on areas of the drop located within close proximity to the pillars and the pinned contact line. These instabilities were due to drop vibrations triggered by the de-pinning process of the receding contact line. They were depicted as bright slit lines on the images and were formed as a result of light penetration from the back-lighting. The receding line was further stretched until the very last moment at t=1.26 ms before the rupture and

collapse of the capillary bridge. This caused the receding line to "snap" and advance to the adjacent pillar.

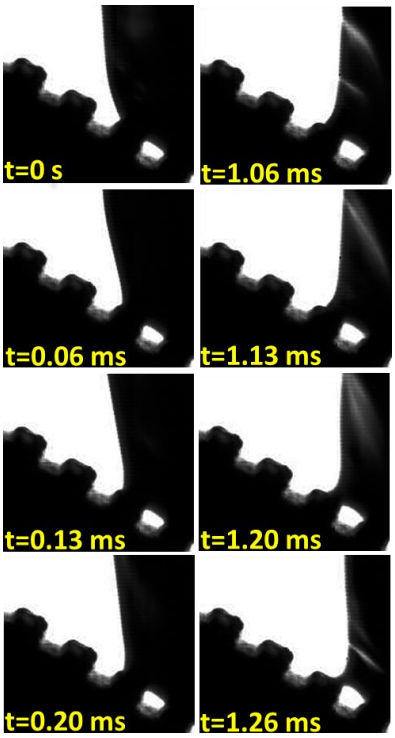

Figure 3: Sequence of high-speed images depicting the initial (0 to 0.2 ms shown in left column) and final events (1.06 ms to 1.26 ms shown in right column) of the microscopic receding line motion on a pillar surface (L=63 µm) while at tilt. The total duration of the receding line motion on the pillar is 1.26 ms. (Image acquired from Yeong *et al.*[19])

The microscopic receding line contact angles on the pillar surface as they progressed from one pillar to another were individually measured for four consecutive pillars and for all pillar surfaces (L= 63 and 120 µm). The angles were then plotted with respect to time as shown in Figure 4. The uncertainty of the angle measurements is estimated to be ±5°. Results show significant variation (90 degrees and above) between the angle measured at the onset of the receding motion (the maximum angle) and the angle measured right before the snapping of the receding line (the minimum angle). After the detachment of the receding line from the pillar, the angle of the contact line would abruptly increase as a new cycle of receding line motion commenced on the adjacent pillar. These receding angle dynamics were observed to be reasonably repeatable for both pillar surfaces. Similar dynamics were observed when the measurement was repeated for a second time on four separate pillars on a different location on the substrates with different inter-pillar distances, i.e. a high receding angle at the onset, followed by a drop in the angles measurement before detachment at a minimum angle. This shows that the measurements are repeatable. The low angles (40-60° for all surfaces) of the pre-snap receding angles suggest a strong affinity of the liquid on the textured pillars. This is hypothesized to be due to the edge effects introduced by the textured pillars.

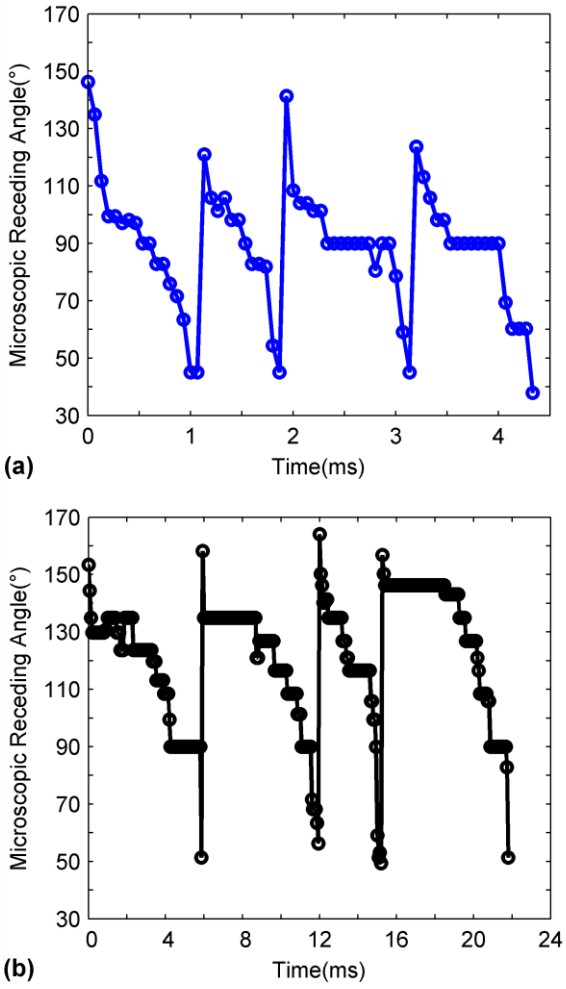

Figure 4: Measurements of the angles of each receding contact line as a function of time for a length of four pillars. Surfaces consist of (a) L= 63 µm (b) L= 120. (Image acquired from Yeong *et al.*[19])

The microscopic receding angles from all four pillars were averaged and plotted with respect to its non-dimensional time, t^*, which was prescribed as $(t-t_o)/T$, where t, t_o and T represents the current, initial and total duration of receding line travel on a single pillar, respectively. In addition, averaged apparent receding angles of the surfaces which were acquired at the apparent (millimeter) length scales were plotted with the microscopic results. This is shown in Figure 5 for all pillar surfaces. The differences in the receding angle between an apparent and microscopic measurement was observed to be substantial. While the initial measurements of the onset receding angle for the apparent and microscopic methods yielded similar

values, it would however diverge as the receding line progressed across the pillar surface.

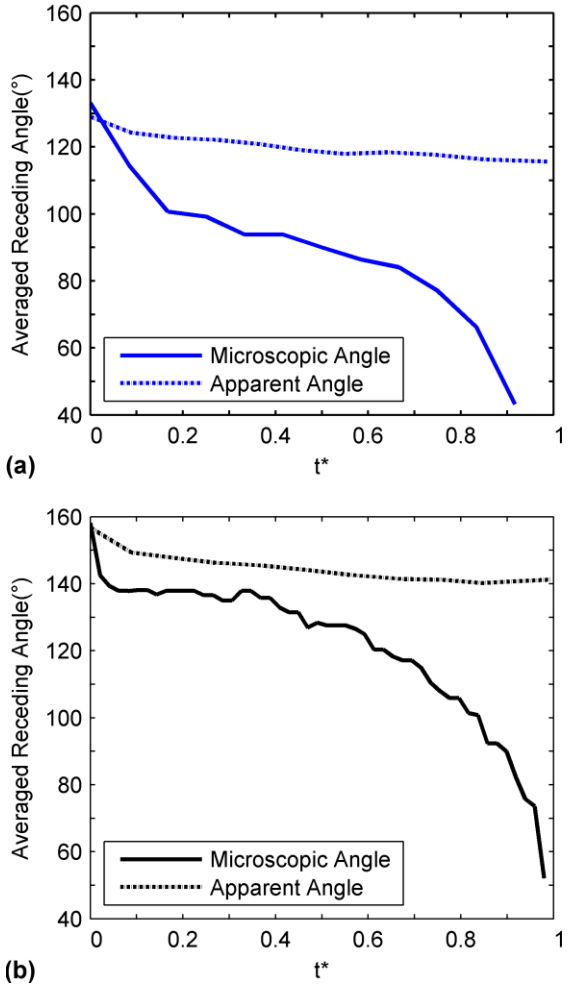

Figure 5 Averaged microscopic and apparent receding angles acquired for a distance of four pillars as a function of non-dimensional time ($t^* = (t-t_o)/T$) where t, t_o and T represents the current, initial and total duration of receding line travel on a single pillar, respectively. (Image acquired from Yeong *et al.*[19])

This was to be expected; the initial receding angle did not involve any complex motions and could be measured without difficulty regardless of length scales. However, once progressed, the macroscopic field of view was insufficient to accurately capture the intricate motions of the three-phase line on each pillar, resulting in a divergence. Therefore, while the fluctuation of the angles from a microscopic measurement would exceed 90°, the variation in apparent angles for all surfaces was consistently limited to within 20°. The variation in magnitude of the apparent angles was consistent with previous studies at similar length scales.[16, 20]

4 CONCLUSIONS

The study of microscopic receding line motion acquired at microsecond time resolution on pillar superhydrophobic surfaces revealed contact line dynamics that were previously not reported. The receding line progressed from the lower edge of a pillar, across the length of the pillar top before "snapping" to advance to the adjacent pillar, creating a "slide-snap" motion. This is in contrast to the "stick-slip" motion that was reported in previous studies. The variation of the microscopic receding angle for this entire sequence of motion was measured to be significant with a difference of approximately 90° between the angles measured at the initial and pre-snap of the receding line. Similar measurements performed at the macroscopic level would only yield a difference of approximately 20°. This observation was consistent for all investigated pillar surfaces with varying L distances.

REFERENCES

[1] A. Cassie et al., T Faraday Soc, 40, 546-551, 1944
[2] R. N. Wenzel, Ind Eng Chem, 28, 988-994, 1936
[3] K. Yeh et al., Langmuir, 24, 245-251, 2008
[4] D. Öner, Langmuir, 16,7777-7782, 2000
[5] S. Wang et al., Adv Mater, 19, 3423-3424, 2007
[6] M. E. Shanahan, Langmuir, 11, 1041-1043, 1995
[7] C. Extrand, Langmuir, 19, 3793-3796, 2003
[8] N. A. Patankar, Langmuir, 26, 7498-7503, 2010
[9] J.W. Krumpfer et al., Faraday Discuss, 146, 103-111, 2010
[10] H. Kusumaatmaja at al., Langmuir, 23, 6019-6032, 2007
[11] B. Mognetti et al., Langmuir, 26, 18162-18168, 2010
[12] L. Gao et al., Langmuir, 22, 6234-6237, 2010
[13] M. Reyssat et al., J Phys Chem B, 113, 3906-3909, 2009
[14] C. Dorrer et al., Beilstein J Nanotechnol, 2, 327-332, 2011
[15] A. T. Paxson et al., Nat Commun, 4, 1492, 2013
[16] K. M. Smyth et al., Surface Innovations, 1, 84-91, 2012
[17] A. Steele, et al., Thin Solid Films, 518, 5426-5431, 2010
[18] L. Cao et al., Langmuir, 23, 4310-4314, 2007
[19] Yeong et al., Sci. Reports, 5, 8384, 2015
[20] J. Zhang et al., Langmuir, 22, 4998-5004, 2006